CELL CYCLE
2021, VOL. 20, NO. 10, 993–1009
https://doi.org/10.1080/15384101.2021.1919825

Taylor & Francis
Taylor & Francis Group

RESEARCH PAPER

Mesenchymal stem cell-derived exosomes containing miR-145-5p reduce inflammation in spinal cord injury by regulating the TLR4/NF-κB signaling pathway

Zhensong Jiang[a] and Jianru Zhang[b]

[a]Department of Spine Surgery, Shandong Provincial Hospital Affiliated to Shandong First Medical University, Jinan City, Shandong Province, China; [b]Department of Health Examination, Jinan Central Hospital Affiliated to Shandong University

ABSTRACT

EXs (Exosomes) secreted by mesenchymal stem cells (MSCs) have the potential to treat spinal cord injury (SCI), this study aimed to further explore the therapeutic effect of EXs on SCI. Firstly, EXs were extracted from MSCs and analyzed with a transmission electron microscope. Next, MSCs with or without the miR-145-5p plasmid were injected into the SCI rat model, and then rat damage was evaluated by BBB score, HE staining and Nissl staining. And then Luciferase experiment verified the targeting relationship between miR-145-5p and TLR4. Furthermore, LPS-induced PC12 cells were established and incubated with Dil-labeled MSC-EXs to explore their effects on cell viability, apoptosis and inflammation through MTT, flow cytometry and ELISA, respectively. In addition, expressions of TLR4/NF-κB signaling pathway related factors were measured by qRT-PCR and Western blot. The results showed that after MSCs were successfully isolated, the existence of EXs in MSCs was confirmed. Moreover, MSC-EXs containing miR-145-5p improved functional recovery and reduced histopathological injury and inflammation in SCI rats. And MSC-EXs promoted miR-145-5p expression in spinal cord tissue and inhibited TLR4/NF-κB pathway activation in SCI rats. MSC-EXs inhibited LPS-induced inflammatory response and activation of the TLR4/NF-κB pathway in PC12 cells. In addition, we also found that miR-145-5p specifically targeted TLR4. TLR4 overexpression significantly reversed the effect of EX-miR-145-5p on maintaining PC12 cell viability, inhibiting apoptosis and inflammatory response, and activating TLR4/NF- κB pathway. In conclusion, mesenchymal stem cell-derived EXs containing miR-145-5p reduce inflammation in spinal cord injury by regulating the TLR4/NF-κB signaling pathway.

ARTICLE HISTORY
Received 2 September 2020
Revised 14 January 2021
Accepted 19 January 2021

KEYWORDS
Mesenchymal stem cell; exosomes; MIR-145-5P; spinal cord injury; TLR4/NF-κB signaling pathway

Introduction

Spinal cord injury (SCI) refers to the injury caused by external force directly or indirectly acting on the spinal cord [1]. SCI, which is rarely cured, often results in physical impairment, loss of perception, and even paralysis, bringing huge pain and a heavy burden to patients and their families [2]. In the past, the medical community believed that the self-repair ability of the spinal cord was extremely poor and that the functional repair of or recovery from SCI was impossible [3]. In the 1980s, scientists discovered nerve cell regeneration in the spinal cord under appropriate conditions, which indicated that SCI might be restored [4]. However, after the onset of severe SCI, patients often suffer from permanent paralysis. Up to now, the treatment of SCI is still a major challenge facing researchers.

More and more studies have found that the inflammatory response after SCI is involved in the injury recovery process [5,6]. At present, some scholars have confirmed the role of inflammatory response in the process and repair of SCI through animal experiments [7]; and some studies have proposed the idea of intervening in the inflammatory response process to promote SCI intervention treatment [8]. Studies have shown that the expression of many genes and post-transcriptional regulation play an important role in SCI-caused inflammatory response [9,10]. Increasing attention has been paid to the inhibitory effect of miRNA on the translation of mRNA, which has emerged as an important method for post-transcriptional regulation [11]. Studies have found that miR-136-5p can affect the inflammatory response following SCI by regulating the

CONTACT Zhensong Jiang jzhensong_zhsongj@163.com

IKKβ/NF-κB/A20 signaling pathway [12]. MiR-145-5p can regulate the inflammatory response of cardiomyocytes induced by hypoxia [13], as well as inhibit the migration, invasion and epithelial-mesenchymal transition of esophageal squamous cell carcinoma cells by regulating the Sp1/NF-κB signaling pathway [14]. Besides, miR-145-5p is also found involved in the process of SCI [15,16]. However, whether miR-145-5p can affect the pathogenesis of SCI by regulating the NF-κB signaling pathway has not yet been reported.

Mesenchymal stem cell (MSC)-exosomes (EXs) are a recently-discovered type of disc-shaped extracellular vesicles with a diameter of 40–100 nm [17]. EXs are rich in nucleic acids, proteins and lipids, and contain abundant biological information [18]. MSC-EXs act on receptor cells to regulate cell activities, and exert an opposite effect on the recovery of bones, cartilages, skin, nerves and other tissues [19]. Studies have shown that MSC-EXs have similar biological functions to MSCs, and are more stable and easy to store [20]. In addition, MSC-EXs contain a variety of miRNAs which can regulate multiple signal transduction pathways [21]. Given the above properties, MSC-EXs have been increasingly employed in orthopedic tissue repair in recent years.

Based on the above evidence, in this study, we transplanted MSC-EXs transfected with miR-145-5p mimic into mice with spinal cord injury to study SCI recovery and the mechanism for the motor function of MSC-EXs, and meantime, to observe the effect of MSC-EXs transfected with miR-145-5p mimic on the biological characteristics of cells stimulated by LPS through *in vitro* cell models. In addition, Studies have shown that the TLR4/NFkB pathway is activated or inhibited in the progression of many diseases. Numerous studies have shown that miRNA can participate in the regulation of endogenous gene signaling pathways, and studies have shown that miR-145-5p promotes TLR4 expression and promotes osteogenic differentiation by activating TLR signaling pathways [22]. However, the effect of miR-145-5p on TLR4/NF-κB signaling pathway in SCI body has not been seen yet. Therefore, in this study, we explore whether EX-miR-145-5p affects the progress of SCI by regulating the TLR4/NF-κB signaling pathway.

Methods

Ethics statement

The animal experiments in this study were approved by the animal ethics committee of Shandong Provincial Hospital and were conducted in accordance with the guidelines of the National Institutes of Health (USA) for animal experiments.

Animals

Eighty one male adult Sprague-Dawley (SD) rats (7 weeks old, 200 ± 20 g) were provided by Hunan Slake Jingda Laboratory Animal Co., Ltd. (http://www.hnsja.com/). All rats were raised for 5 days in an SPF environment before the experiment.

MSC isolation and culture

One adult rat was selected for isolation of MSCs. In short, the bone marrow of the SD rat was isolated, and the cells were washed and suspended in the culture medium. MSCs were cultured on 75 cm^2 tissue culture flasks in DMEM medium (Gibco, USA) containing 20% fetal bovine serum (FBS, Gibco, USA) and penicillin/streptomycin (15070063, Gibco, USA). After 48 h of culture, the medium was replaced with a fresh medium to remove non-adherent cells. When reaching 90% confluence, the cells were digested with trypsin and then passaged.

Transfection

To investigate the effects of miR-145-5p on MSC-EXs, a transfection assay was used for experimental proof. Briefly, miR-145-5p mimic was purchased from Thermo Fisher SCIENTIFIC (MIMAT0000851), and its sequence (5 -UCCCUAAGGACCCUUUUGACCUG-3) was synthesized by Guangzhou RiboBio Co., Ltd. Then it was transfected into MSCs (3×10^5 cells) using Lipofectamine™ 2000 transfection reagent (Invitrogen, Carlsbad, California, USA). For comparison, miR-145-5p negative control (NC) transfected cells served as a mimic control. To investigate the effects of TLR4 on PC12 cells, the TLR4 overexpression vector was transfected into

PC12 cells using Lipofectamine™ 2000 transfection reagent.

EX isolation from transfected MSCs

Forty eight h after transfection, EXs were isolated from MSCs. A 0.2 mm filter was used to filter the supernatant of large debris and dead cells collected in the cultured MSCs. Then small cell debris in the cell supernatant was removed by centrifugation at 10,000 × *g* for 30 minutes, and then the supernatant was centrifuged again at 100,000 × *g* for 3 h. We detected the expressions of EV markers CD9 and CD63 by Western blotting (WB). The size distribution of EXs was determined by nanoparticle tracking analysis. The morphology of EXs was confirmed under a transmission electron microscopy at × 1,000 magnification.

Rat SCI model establishment and groups

The rats were randomly divided into 5 groups (n = 16): Sham, Model, Model+PBS, Model+EX-miR-NC, and Model+EX-miR-145-5p groups. The rats in the Model group were used to established SCI model. Briefly, the rats were anesthetized by intraperitoneal injection with 10% chloral hydrate (0.33 mL/kg). Subsequently, the rats were fixed on the operating table, and an incision was made along the midline of the back to expose the spinal cord. Thereafter, laminectomy was performed at the T9/10 position. In the Sham group, only an incision was made along the midline of the back of the rats to expose the spinal cord. The Model+EX-miR-NC and Model+EX-miR-145-5p groups were set up to evaluate the therapeutic effect of MSC-derived EX-miR -145-5p on the recovery of motor function after SCI. In brief, 30 min after the operation, the rats in both groups were injected with EXs isolated from MSCs in the miR-NC and miR-145-5p groups (100 μg of total EX protein was precipitated in 0.5 mL of PBS, equivalent to 1×10^{10} particles) via the tail vein. The Model+PBS group served as the Model+EX-miR-NC group: Rats in the Model+PBS group received PBS injection of an equal volume of 0.5 ml. On days 1, 3, 7, 14, 21, and 28 after the operation, the rats in each group were examined by spontaneous activity scores and horizontal step walking tests. Finally, the rats were euthanized at a predetermined time point, and spinal cord tissue was collected for testing.

Basso, Beattie, and Bresnahan (BBB) score

According to previous publications [23,24], the BBB score was used to evaluate the motor function of each group of rats on days 1, 3, 7, 14, 21, and 28 after the injury. The score ranged from 0 (indicating complete paralysis) to 21 (indicating normal movement). Three experienced researchers who were unaware of the grouping of the animals in this study independently observed and evaluated the movement of the rats. The final score of each animal was obtained by averaging the values of the three researchers.

Hematoxylin and eosin (HE) staining

Histopathological observation was performed on the spinal cord of the rats 28 days after operation. The spinal cord of the rats was placed in 4% formaldehyde solution for 24 h, and then decalcified with 15% EDTA decalcification solution. The decalcification was regularly checked with acupuncture samples. There is no resistance when the pin is inserted into the tissue, indicating that decalcification was complete, and then the decalcification was terminated. The specimen was washed with running water, dehydrated with alcohol, and transparentized with xylene. Then after the tissues were dewaxed and embedded, 5 μm thick tissue sections were made. After that, the tissue sections were stained using the HE staining kit (C0105, Beyotime Biotechnology, China). In short, the tissue sections were stained with hematoxylin for 5 min, differentiated with hydrochloric acid ethanol for 30 s, and stained with eosin for 2 min. Then the tissue sections were dehydrated, transparentized and mounted, and finally, the pathological changes of bone tissue were observed under a microscope (CKX31, Olympus, Japan) at a magnification of × 200.

Nissl staining

After the spinal cord of the rats was placed in 4% formaldehyde solution for 24 h, 20% sucrose and 30% sucrose which were prepared with 100%

sucrose (S112226, Aladdin) and ddH_2O were used to successively incubate the spinal cord at 37°C. Then the spinal cord tissues were sectioned, soaked in chloroform for 30 min, and incubated with 100% acetone (650501, Sigma-Aldrich). After further incubation with gradient doses of ethanol, the tissue sections were stained with tar purple (C861450, Macklin, Shanghai, China) for 10 min. Then the tissue sections were rehydrated with gradient doses of ethanol and incubated with xylene for 5 min until transparent. Finally, after sealing with neutral gum, the image of the tissue slice was observed and collected under the microscope at a magnification of × 200.

PC12 cell treatment

PC12 cells were obtained from the American Type Culture Collection (ATCC; Rockville, MD, USA). For normal culture, the PC12 cells were cultured in the DMEM (30–2002, ATCC) contains 10% FBS (16140063, Gibco, MA, USA) at 37°C in a humid atmosphere with 5% CO_2. The cells were divided into four groups, namely, Control, LPS, LPS+EX-miR-NC and LPS+EX-miR-145-5p groups.

For LPS-induced inflammatory models, the cells were treated with 5 μg/ml LPS (Sigma-Aldrich, MA, USA), followed by PBS treatment for 24 h.

For EX-miR-NC and EX-miR-145-5p treated cell models, firstly, MSC-EXs were fluorescently labeled, and 4 mg/mL Dil solution was added to PBS (1:200) and incubated. Ultracentrifugation was used to remove excess dye in the fluorescently labeled MSC-EXs at 100,000 × *g* at 4°C for 1 h, and the pellets were resuspended in PBS and washed 3 times. Then 3×10^5 PC12 cells were incubated with 10 μg of Dil-labeled MSC-EXs for 48 h. Afterward, the cells were washed with PBS and fixed with 4% paraformaldehyde. Then the absorption was observed with a confocal laser microscope. PC12 cells in the Control group were incubated for 48 h in the medium without MSC-EX.

In the LPS+EX-miR-NC and LPS+EX-miR-145-5p groups, After PC12 cells were transferred to 5 μg/ml LPS for 12 h, 10 μg/mL EXs extracted from MSCs with miR-145-5p mimic or mimic control were used to treat PC12 cells for 24 h at 37°C.

Luciferase activity assay

For luciferase activity assay, the sequence of TLR4 containing the binding sites for miR-145-5p was: 5 -AAATTCAGTTGTCAAAACTGGAA-3 , and the 3 -UTR sequence of WT TLR4 was inserted into the pmirGLO Vector (Promega, Madison, Wisconsin, USA) with XhoI and SacI double digestion. Both sequences were used to construct the recombinant dual-luciferase reporter vector. Meanwhile, The plasmid containing the MUT TLR4 sequence was generated through DNA synthesis (Sangon Biotech Co. Ltd., Shanghai, China). After that, the pmirGLO vector containing WT or MUT TLR4 sequence was co-transfected with miR-145-5p mimic into cells by using Lipofectamine™ 2000 (Invitrogen, USA). After incubation for 48 h, a Luciferase reporter gene detection kit (RG088S, Beyotime Biotechnology, China) was used to measure the relative luciferase activity of cells.

ELISA assay

The spinal cord of rats and PC12 cells were collected to detect the contents of IL-6, TNF-α and IL-1β. In short, the contents of IL-6, TNF-α and IL-1β were detected by IL-6, TNF-α and IL-1β ELISA detection kits (PI328, PT516, PI303, Beyotime Biotechnology, China) separately, 100 μl of sample was added to a 96-well plate with primary antibodies pre-coated plate, and two duplicate wells per well were set, and incubate at room temperature for 120 min. And then the plates were washed three times with wash solution. Afterward, 100 μl of diluted horseradish peroxidase-labeled streptavidin was added to each well, and incubated at room temperature for 30 min, and subsequently, 100 μl of coloring substrate TMB solution (P0209, Beyotime Biotechnology, China) was added to each well and incubated at room temperature for 10 min in the dark. Then 50 μl of stop solution 2 N H_2SO_4 was used to stop the color reaction. Finally, a microplate reader (SPECTROstar® *Nano*, BMG LABTECH, USA) was used to detect the OD value of each well at 450 nm and 570 nm.

Cell viability detection

An MTT kit (M8180/M1020, Solarbio, China) was used to detect the viability of PC12 cells. The cells were inoculated into 96-well plates, and after reaching 80% confluence, the cells were added with 10 μL of MTT solution and incubated for 4 h with 5% CO_2 at 37°C. Finally, the absorbance of each well was detected at 550 nm using a microplate reader (BMG Labtech, Germany).

Cell apoptosis

In order to investigate the effect of EX-miR-145-5p and TLR4 on the apoptosis of PC12 cells, an Annexin V-FITC Apoptosis Detection Kit (C1062S, Beyotime Biotechnology, USA) was used to detect cell apoptosis. Briefly, after collecting the cell supernatant, 195 μl of Annexin V-FITC binding solution and 5 μl of Annexin V-FITC were added to cell supernatant. Then the cells were incubated with 10 μl of propidium iodide staining solution at 25°C for 20 min. Finally, apoptosis was detected by flow cytometry (FACSCaliburTM; BD Biosciences, San Jose, CA, USA).

Quantitative reverse transcription-polymerase chain reaction (qRT-PCR)

Total RNA was extracted from cells with Trizol reagent (R0016, Beyotime Biotechnology, USA) at 25°C. Of note, when RNA precipitation was dissolved in water, it needed to be quickly operated on ice. After the RNA was identified and purified, a PrimeScript RT kit (RR037A, Takara, China) was used to reverse-transcribe it into cDNA. SYBR Green PCR Master Mix (D7268M, Beyotime Biotechnology, USA) was used to quantitate the mRNA expression levels. PCR amplification system was prepared as follows: 5 μl of 2 × SYBR Green master mix, 2 μl of nuclease-free water, 1 μl of cDNA, and 0.5 μl of Forward Primer and 0.5 μl of Reverse Primer were mixed together. The PCR cycle system of the ABI7500 system (Applied Biosystems) was set as follows: Pre-denaturation at 95°C for 10 min; then PCR reaction at 95°C for 3 s, and at 60°C for 30 s, for a total of 50 cycles. The $2^{-\Delta\Delta CT}$ method was used to calculate the changes of relative mRNA expression levels [25]. Primer sequences of all genes are listed in Table 1. U6 and β-actin internal reference genes were used to normalize qRT-PCR data.

Western blotting

The tissues and cells were washed with cold PBS, and then lysed with the lysis buffer (R0278, Sigma-Aldrich, USA). Then, the supernatant was collected in a new tube and placed on ice, and the precipitate was discarded. A QuantiPro ™ BCA detection kit (QPBCA, Sigma-Aldrich, USA) was used to measure the protein concentration. The protein was incubated with primary antibodies: CD9 (ab92726, 25 kDa, Abcam, USA), CD63 (ab134045, 26 kDa, Abcam, USA), TLR4 (sc-293072, 95 kDa, Santa Cruz, USA), p-P65 (ab86299, 60 kD, Abcam, USA), p65 (ab16502, 64 kD, Abcam, USA), p-IκBα (#9246, 40 kD, CST, USA), IκBα (#9246, 39 kD, CST, USA) and β-actin (ab8226, 42kDa, Abcam, USA) at 4°C overnight separately, among which β-actin served as an internal reference. Next, the membranes were incubated for 2 h with corresponding fluorescent secondary antibodies (Protein tech, USA). Next, a chemiluminescent Biotin-labeled Nucleic Acid Detection Kit (D3308, Beyotime Biotechnology, China) was used to measure the protein bands. Finally, a FLoid™ Cell Imaging Station (Thermo Fisher Scientific, Massachusetts, US) was used to record and analyze the specific protein brands.

Statistical analysis

Statistical analysis was performed using Graphpad prism 8.0, and the measurement data are

Table 1. Primers used in real-time PCR analysis.

Gene	Primer sequence
miR-145-5p	Forward: 5 -GTCCAGTTTTCCCAGGAATCCC-3
	reverse: 5 - TGTCGTGGAGTCGGCAATTG –3′
TLR4	Forward:5 - GTCATGCTTTCTCACGGCCT-3
	reverse:5 -AATTGTCTCAATTTCACACCTGGAT-3′
β-actin	Forward:5 - GTGACGTTGACATCCGTAAAGA –3
	reverse: 5 - GCCGGACTCATCGTACTCC –3′
U6	Forward:5 - GCTTCGGCAGCACATATACTAA –3
	reverse: 5 - CGAATTTGCGTGTCATCCTT –3′
P65	Forward:5 - CGTTCGAGCAAATCCAGAAAGTG-3
	reverse: 5 - AGGAACTCACTGGCTCCTTC –3′
IκBα	Forward:5 - AACAACCTGCAGCAGACTCC-3
	reverse: 5 - CACAATAGAATGCTCGGGGC-3′

expressed as mean ± standard deviation. The independent samples *t* test was used for comparison between two groups. One-way analysis of variance was used for comparison among multiple groups, and Bonferroni or Dunnett test was used for post-hoc comparison. To ensure the reproducibility of the results, each experiment was repeated 3 times. The difference was recognized as statistically significant when $p < 0.05$.

Results

The identification of EXs around MSCs and the expression level of miR-145-5p were detected in MSC-EXs

After MSCs were successfully isolated and cultured, the formation of EXs was analyzed by transmission electron microscopy and nanometer scale. Transmission electron microscopy showed that there were spherical vesicles in the EXs which appeared to be typically goblet shaped (Figure 1a). EXs were identified by Western blotting, and the results showed that specific EXs such as CD63 and CD9 were positive in mesenchymal EXs, which further confirmed the existence of EXs, WB detected the expression levels of CD63, CD9 and TSG101 in the whole cell lysate. The results showed that the expression levels of CD63, CD9 and TSG101 were less than those in the EX-miR-NC and EX-miR-145-5p groups (Figure 1b). After transfecting miR-145-5p NC and miR-145-5p mimic into MSCs separately, we used qRT-PCR to detect the expression level of miR-145-5p in MSC-EXs of each group. The results showed that the expression level of miR-145-5p in MSC-derived EXs with miR-145-5p mimic increased significantly (Figure 1c, $p < 0.001$).

MSC-EXs containing miR-145-5p improved functional recovery and reduced histopathological injury and inflammation in SCI rats

We further established an SCI rat model to explore the effects of injection with MSC-EXs on SCI model rats. The BBB score was used to evaluate the hind limb function recovery of rats. The hind limb function of rats in the Model group was severely damaged after surgery compared with the Sham group; the hind limb function recovery of mice in the EX-miR-145-5p-NC group was better than that of mice in the Model+PBS group; and the hindlimb function recovery of EX-miR-145-5p group rats was the most significant (Figure 2a, $p < 0.01$, $P < 0.001$). These results suggest that injection with MSC-EXs can promote functional recovery in SCI rats. After the rat spinal cord tissue was collected 28 days after the operation, HE staining and histopathological observation were conducted. The results showed that compared with the Sham group (rats in the sham group showed a complete spinal cord structure, normal neuronal morphology, clear cells and outlines, and no inflammatory cell infiltration), the spinal cord tissue of rats in the Model group (rats in the Model group showed the spinal cord is incomplete and its organization is disordered.

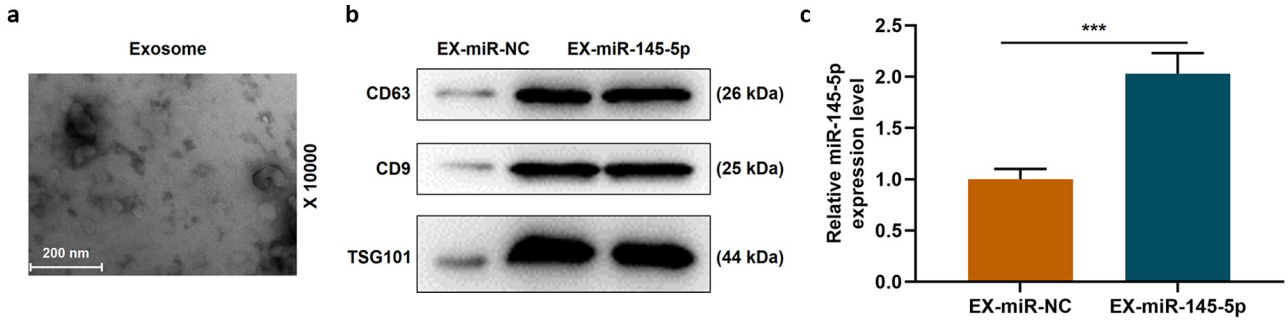

Figure 1. The identification of EXs around MSCs and the expression level of miR-145-5p were detected in MSC-EXs.

(a) After MSCs were successfully isolated and cultured, the formation of EXs was analyzed by transmission electron microscopy and nanometer scale. (b) EXs were identified by Western blotting to detect the expression of CD63 and CD9. (c) MiR-145-5p NC and miR-145-5p mimic were transfected into MSCs separately, and qRT-PCR was used to detect the expression level of miR-145-5p in MSC-EXs of each group (n = 3, ***$P < 0.001$, vs. EX-miR-NC)

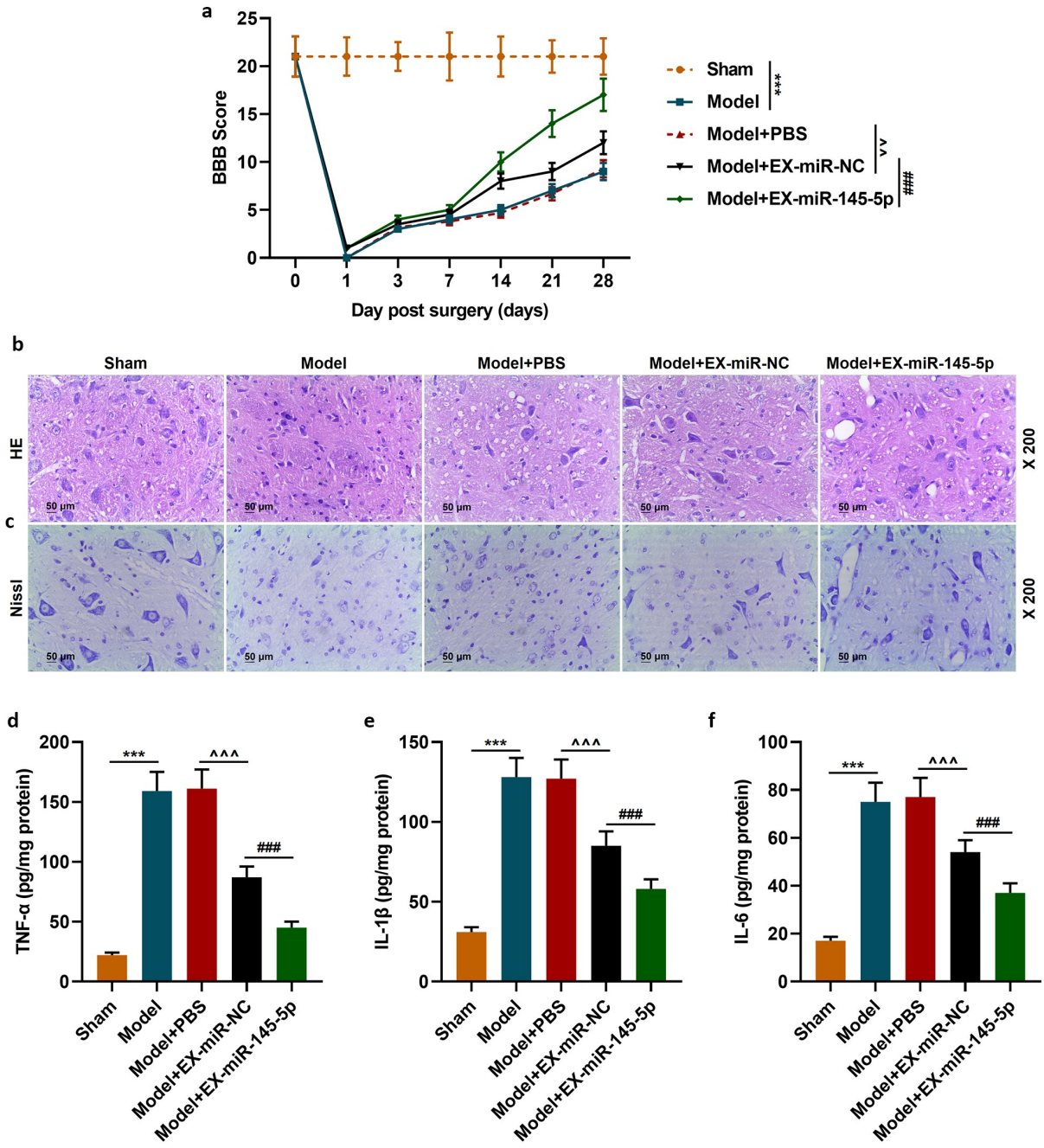

Figure 2. MSC-EXs (EX) containing miR-145-5p improved functional recovery and reduced histopathological injury in SCI rats. (a) The BBB score was used to evaluate the hind limb function recovery of rats. (b) The rat spinal cord tissue was collected 28 days after the operation for HE staining and histopathological observation. (c) The rat spinal cord tissue was collected 28 days after the operation for Nissl staining. ELISA was used to detect the expressions of inflammatory factors TNF-α (d), IL-1β (E) and IL-6 (f) in spinal cord tissue, and to explore the effect of MSC-EXs on the inflammation of SCI rats. (n = 3, $^{***}P < 0.001$, vs. Sham group; $^{\#\#\#}P < 0.001$, vs. Model+EX-miR-NC group; $^{\wedge\wedge}P < 0.01$, $^{\wedge\wedge\wedge}P < 0.001$, vs. Model+PBS group)

The cell nucleus division even disappears. The gap between cells and blood vessels is enlarged, and inflammatory cell infiltration is obvious) was severely damaged; EX-miR-145-5p-NC (rats in the Model + EX-miR-145-5p-NC group showed that the disorder of tissue structure was improved, the space between cells and blood vessels was reduced, and the infiltration of inflammatory cells was reduced) and EX-miR-145-5p (rats in the Model + EX-miR-145-5p group showed less inflammatory cell infiltration and more complete tissue structure) both could reduce spinal cord

injury, and EX-miR-145-5p had a significantly better repairing effect on injured spinal cord (Figure 2b). In addition, after the rat spinal cord tissue was collected 28 days after the operation, Nissl staining was performed. The results showed that compared with the Sham group, the rat spinal cord tissue of rats in the Model group had obvious neuronal apoptosis; both EX-miR-145-5p-NC and EX-miR-145-5p could reduce nerve cell apoptosis, and the neuroprotective effect EX-miR-145-5p was the most significant (Figure 2c). These results indicate that MSC-EX injection can reduce tissue injury in SCI rats. Then, we used ELISA to detect the expressions of inflammatory factors TNF-α, IL-1β and IL-6 in spinal cord tissue, and explored the effect of MSC-EXs on the inflammation in SCI rats. It was found that compared with the Sham group, the spinal cord tissue of Model group rats displayed significantly higher levels of TNF-α, IL-1β and IL-6. Meantime, both EX-miR-145-5p-NC and EX-miR-145-5p could reduce the release of TNF-α, IL-1β and IL-6, and EX-miR-145-5p had a more significant inhibitory effect on inflammation (Figure 2d-F, $P < 0.001$). This indicates that MSC-EXs can reduce the inflammatory response in SCI rats.

MSC-EXs could promote the expression of miR-145-5p in spinal cord tissue and inhibit the activation of TLR4/NF- κB pathway in SCI rats

QRT-PCR was used to detect the expression of miR-145-5p in injured spinal cord tissue of mice in the Sham, Model, Model+EX-miR-145-5p-NC, Model+PBS and Model+EX-miR-145-5p groups. We found that compared with the Sham group, the expression of miR-145-5p in the spinal cord tissue of Model group rats was significantly reduced. Meanwhile, EX-miR-145-5p-NC and EX-miR-145-5p both increased the expression of miR-145-5p in the spinal cord tissue, and EX-miR-145-5p injection had the most significant promoting effect on miR-145-5p levels in spinal cord tissue (Figure 3a, $p < 0.001$). Then, qRT-PCR and Western blot were used to detect the expressions of TLR4, p-P65, p65, p-IκBα and IκBα in the spinal cord tissues of mice in each group. The results showed that compared with the Sham group, the expression of TLR4 in the spinal cord tissue of Model group rats was significantly increased, accompanied by activated NF-κB pathway. At the same time, both EX-miR-145-5p-NC and EX-miR-145-5p could effectively inhibit the activation of TLR4/NF-κB pathway, and EX-miR-145-5p had a more significant inhibitory effect on TLR4/NF-κB pathway activation (Figure 3b-F, $P < 0.01$, $P < 0.001$), which suggests that MSC-EXs can affect TLR4/NF-κB activation in the pathogenesis of SCI.

MSC-EXs inhibited LPS-induced inflammatory response and activation of the TLR4/NF-κB pathway in PC12 cells

We further explored the effect of exosomal miR-145-5p on spinal cord injury through in *vitro* experiments. We constructed a cell injury model by treating PC12 cells with LPS and explored the effect of exosomal miR-145-5p on the biological characteristics of LPS-induced PC12 cell. Firstly, a fluorescence microscope was used to observe the changes in the uptake of fluorescently labeled EXs by PC12 cells and the Control group. The results showed that after 48 hours of incubation, Dil labeled EXs existed in more than 56% of PC12 cells in the EX-treated group, which shows that we have successfully obtained PC12 cells infected with EXs (Figure 4a). QRT-PCR was then conducted to detect the expression of miR-145-5p in PC12 cells, and the results showed that both EX-miR-145-5p-NC and EX-miR-145-5p could reduce the inhibitory effect of LPS on the viability of PC12 cells, and EX-miR-145-5p had a more significant protective effect on PC12 cells (Figure 4b, $p < 0.001$). Then, we used the MTT assay to detect cell viability. As shown in Figure 4c, both EX-miR-145-5p-NC and EX-miR-145-5p could reduce the inhibitory effect of LPS on PC12 cell viability, and the protective effect of EX-miR-145-5p on PC12 cells was more significant ($P < 0.01$, $P < 0.001$). Flow cytometry staining was performed to detect cell apoptosis, and we found that both EX-miR-NC and EX-miR-145-5p could reduce the apoptosis of PC12 cells induced by LPS, and EX-miR-145-5p had a more significant inhibitory effect on PC12 cell apoptosis (Figure 4d-E, $P < 0.001$). Likewise, ELISA was used to detect the contents of TNF-α, IL-1β and IL-6 in the cell supernatant.

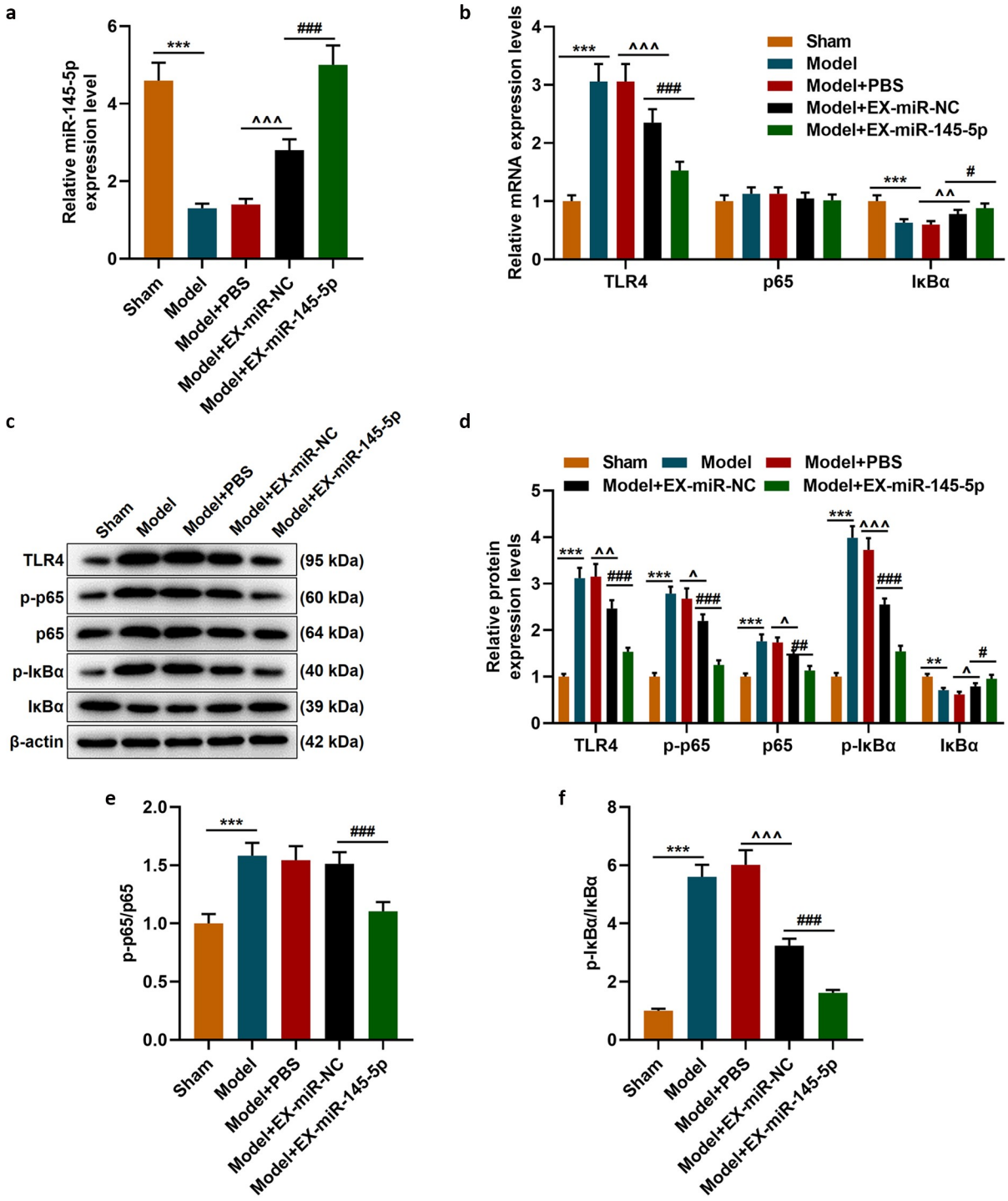

Figure 3. MSC-EXs could promote the expression of miR-145-5p in spinal cord tissue and inhibit the activation of TLR4/NF- κB pathway in SCI rats.

(a) QRT-PCR was used to detect the expression of miR-145-5p in injured spinal cord tissue of rats in the Sham, Model, Model+EX-miR -145-5p-NC, Model+PBS and Model+EX-miR-145-5p groups. (b) QRT-PCR and Western blot (c–f) were used to detect the expressions of TLR4, p-P65, p65, p-IκBα and IκBα in the spinal cord tissues of rats in each group. (n = 3, $^{***}P < 0.001$, vs. Sham group; $^{\#}P < 0.05$, $^{\#\#\#}P < 0.001$, vs. Model+EX-miR-NC group; $^{\wedge\wedge}P < 0.01$, $^{\wedge\wedge\wedge}P < 0.001$, vs. Model+PBS group)

Figure 5a-c showed that both EX-miR-NC and EX-miR-145-5p could inhibit the production of inflammatory factors induced by LPS, and EX-miR-145-5p had a more significant inhibitory effect on the production of inflammatory factors ($P < 0.001$). QRT-PCR and Western blot were used to detect the expression levels of TLR4, p-P65, P65, p-IκBα and IκBα in the cells. The

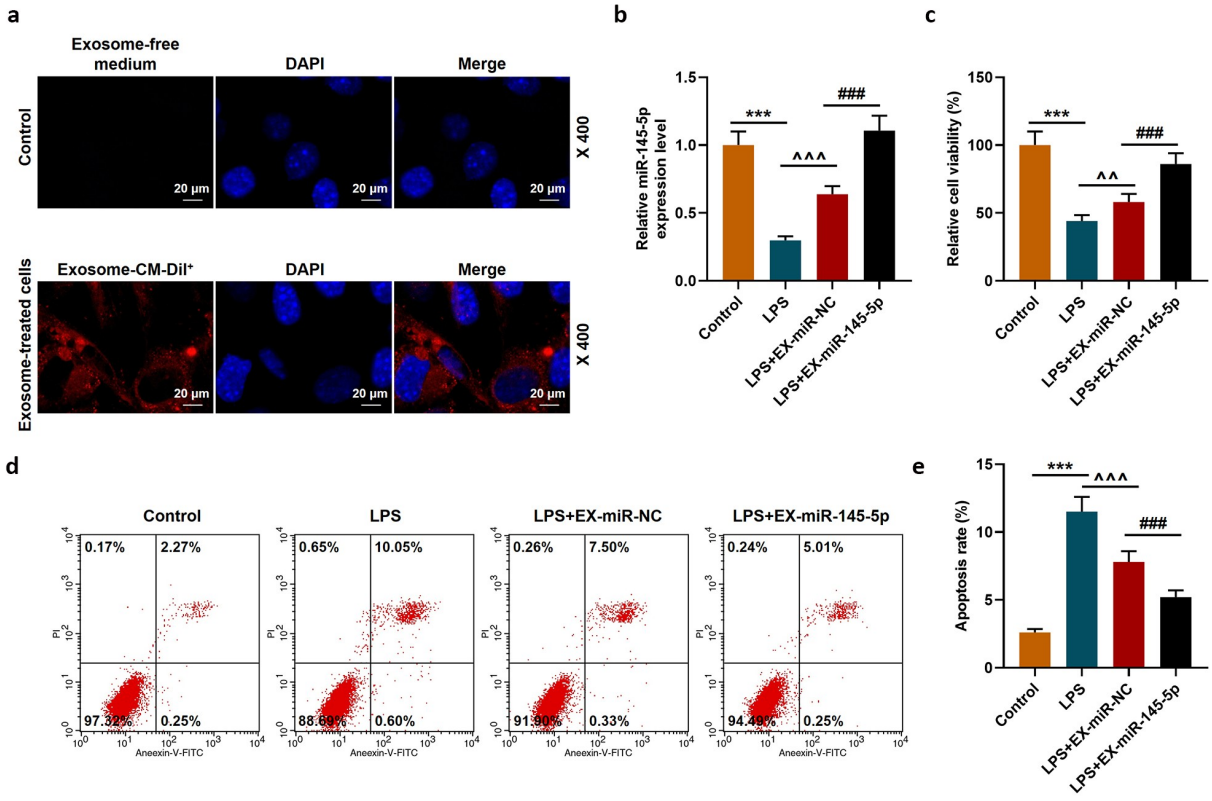

Figure 4. MSC-EXs could inhibit the effect of LPS inhibition ofon inhibiting miR-145-5p expression, cell viability and apoptosis in PC12 cells.

(a) A cell injury model was constructed by treating PC12 cells with LPS. A fluorescence microscope was used to observe the changes in the uptake of fluorescently labeled EX by PC12 cells and the Control group. (b) QRT-PCR was used to detect the expression of miR-145-5p in PC12 cells. (c) MTT was used to detect the viability of PC12 cells treated with LPS. (d,e) Flow cytometry staining was used to detect cell apoptosis. (n = 3, $^{***}P < 0.001$, vs. Control group; $^{\#\#\#}P < 0.001$, vs. LPS+EX-miR-NC group; $^{\wedge\wedge}P < 0.01$, $^{\wedge\wedge\wedge}P < 0.001$, vs. LPS group)

results were shown in Figure 5d-H: EX-miR-NC and EX-miR-145-5p could both inhibit LPS-induced increase in TLR4 expression and activation of NF-κB pathway, and EX-miR-145-5p had a more significant inhibitory effect on TLR4/NF-κB pathway activation ($P < 0.001$).

MiR-145-5p could specifically target TLR4 and inhibit TLR4 expression

The target gene prediction database TargetScan 7.1 showed that miR-145-5p could specifically target TLR4 (Figure 6a). Then dual luciferase assay was used to further verify the targeting relationship between miR-145-5p and TLR4, and the results showed that overexpression of miR-145-5p could significantly inhibit the fluorescent activity of TLR4 (Figure 6b, $p < 0.001$). Next, the expression of TLR4 in cells was measured. As shown in Figure 7a-7c, transfection with TLR4 overexpression plasmid could significantly reverse the inhibitory effect of EX-miR-145-5p on TLR4 expression in PC12 cells ($P < 0.001$).

TLR4 overexpression significantly reversed the effect of EX-miR-145-5p on maintaining PC12 cell viability, inhibiting apoptosis and inflammatory response, and activating TLR4/NF- κB pathway

The effect of TLR4 overexpression on the function of exosomal miR-145-5p in improving the inflammatory response of PC12 cells was further explored. Firstly, the MTT method was used to detect cell viability, and the results showed that TLR4 overexpression could significantly reverse the protective effect of EX-miR-145-5p on PC12 cell viability (Figure 7d, $p < 0.001$). Next, apoptosis was detected by Flow cytometry, and as shown in Figure 7e- 7f, TLR4 overexpression could

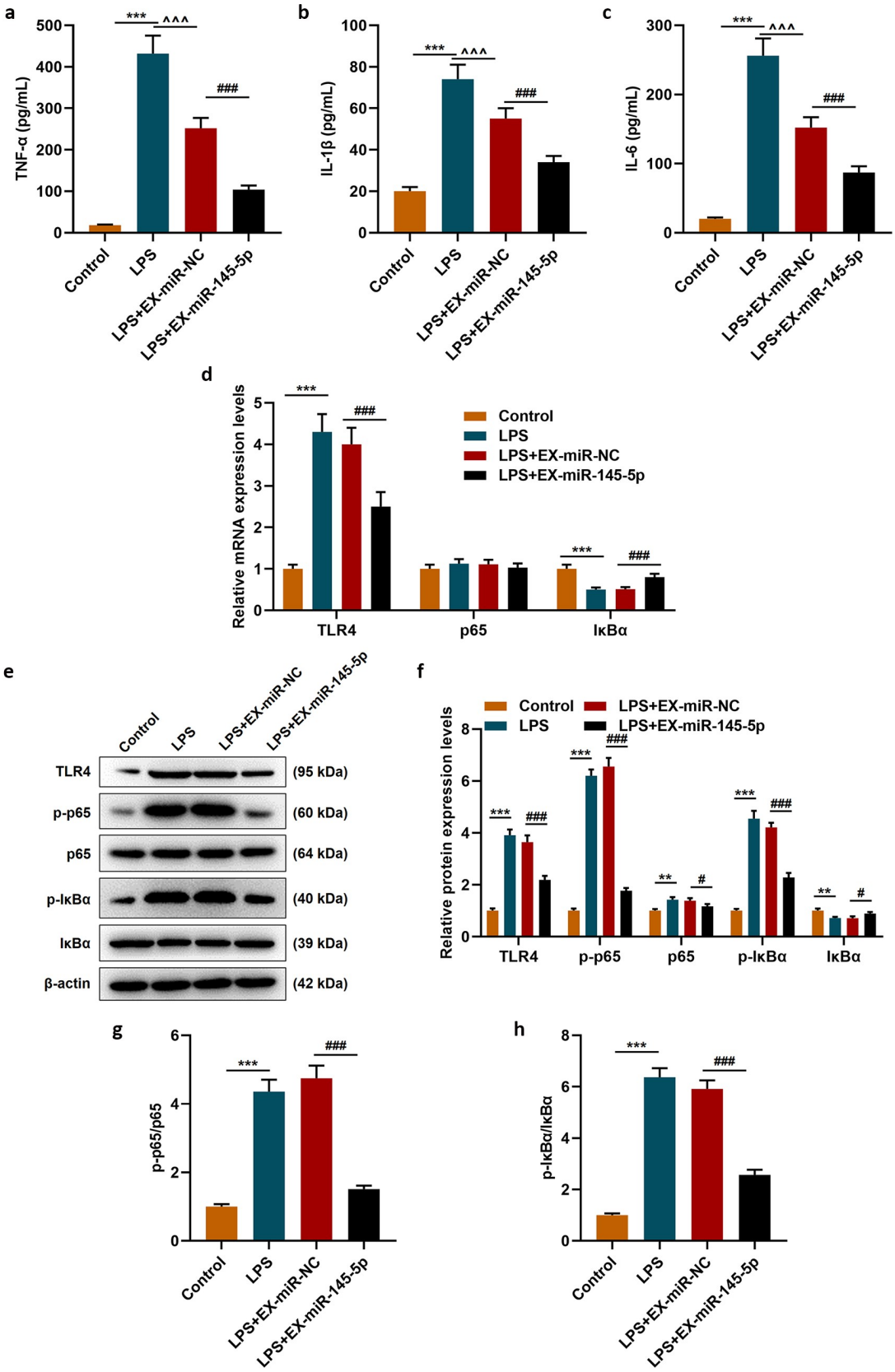

Figure 5. MSC-EXs inhibited LPS-induced inflammatory response and activation of the TLR4/NF-κB pathway in PC12 cells.

ELISA was performed to detect the contents of TNF-α (a), IL-1β (b) and IL-6 (c) in the cell supernatant. QRT-PCR (d) and Western blot (E-H) were used to detect the expression levels of TLR4, p-P65, P65, p-IκBα and IκBα in the cells. (***$P < 0.001$, vs. Control group; ##$P < 0.01$, ###$P < 0.001$, vs. LPS+EX-miR-NC group; ^^^$P < 0.001$, vs. LPS group)

Figure 6. MiR-145-5p could specifically target TLR4 and inhibit TLR4 expression.
(a) The target gene prediction databse TargetScan 7.1 was used to predict the target relationship between miR-145-5p and TLR4. (b) The dual luciferase assay was used to further verify the targeting relationship between miR-145-5p and TLR4. (n = 3, $^{\Delta\Delta\Delta}P<0.001$, vs. miR-NC group)

significantly reverse the inhibitory effect of EX-miR-145-5p on PC12 cell apoptosis ($P < 0.001$). Moreover, ELISA was used to detect the expressions of TNF-α, IL-1β and IL-6, and as shown in Figure 8a- 8c, overexpression of TLR4 could significantly reverse the effect of EX-miR-145-5p on inhibiting PC12 cells from producing inflammatory factors ($P < 0.001$). Finally, the expression levels of p-P65, P65, p-IκBα and IκBα in cells were detected by qRT-PCR and Western blot. The results showed that TLR4 overexpression could significantly reverse the inhibitory effect of EX-miR-145-5p on NF-κB pathway activation (Figure 8d- 8h, $P < 0.001$).

Discussion

SCI is a serious and complex clinical disease characterized by neuronal damage, axon destruction and demyelination [26]. Due to its high incidence and complex pathological processes, there is still a lack of effective clinical treatment methods. Research in recent years has shown that EX is involved in many physiological and pathological processes, including lactation and immune response [27]. In addition, EX is also involved in the occurrence and development of certain diseases, such as neurodegeneration, liver disease and tumors [28]. At present, EX-mediated cell-to-cell communication has received widespread attention [29]. EXs carry genetic materials (miRNA, mRNA, etc.) into target cells through transport and endocytosis, thereby exerting biological effects. Multiple studies on SCI have found that miR-17-92 in EXs can target the signaling pathway protein Akt, mammalian target of rapamycin, and glycogen synthase kinase-3β, promote Akt phosphorylation, and activate the corresponding signal pathways to promote axon growth and remyelination [30,31]. In addition, Lankford et al. found that MSCs mainly repaired spinal cord injury by secreting EXs [32]. Sun et al. injected human umbilical cord-derived MSC EXs intravenously into a rat model of spinal cord injury, and found that MSC-EXs can down-regulate inflammatory mediators such as TNF-α, IL-1α, IL-6 and γ-interferon to improve the recovery of nerve function after spinal cord injury [33]. Huang et al. injected MSC-EXs intravenously in a rat model of spinal cord injury and found that MSC-EXs can up-regulate the expressions of anti-inflammatory and anti-apoptotic proteins, reduce the release of pro-apoptotic proteins and pro-inflammatory mediators, and inhibit cell apoptosis [34].

Studies have shown that the down-regulation of miR-145-5p in injured spinal cord is related to astrocyte hyperplasia and glial scar formation after spinal cord injury [15]. Global screening of miRNA expression changes under different muscle atrophy conditions in SCI rats showed that miR-145-5p expression was down-regulated after denervation or starvation [16]. Studies have found that EXs derived from adipose stem cells (ADSCs) can deliver miR-122 to liver cancer cells, and regulate the expression of its target genes cyclin G1 and insulin-like growth factor receptor 1, making liver cancer cells more sensitive to chemotherapy drugs [35]. In a rat model of primary brain tumor, after intratumor injection with MSC-

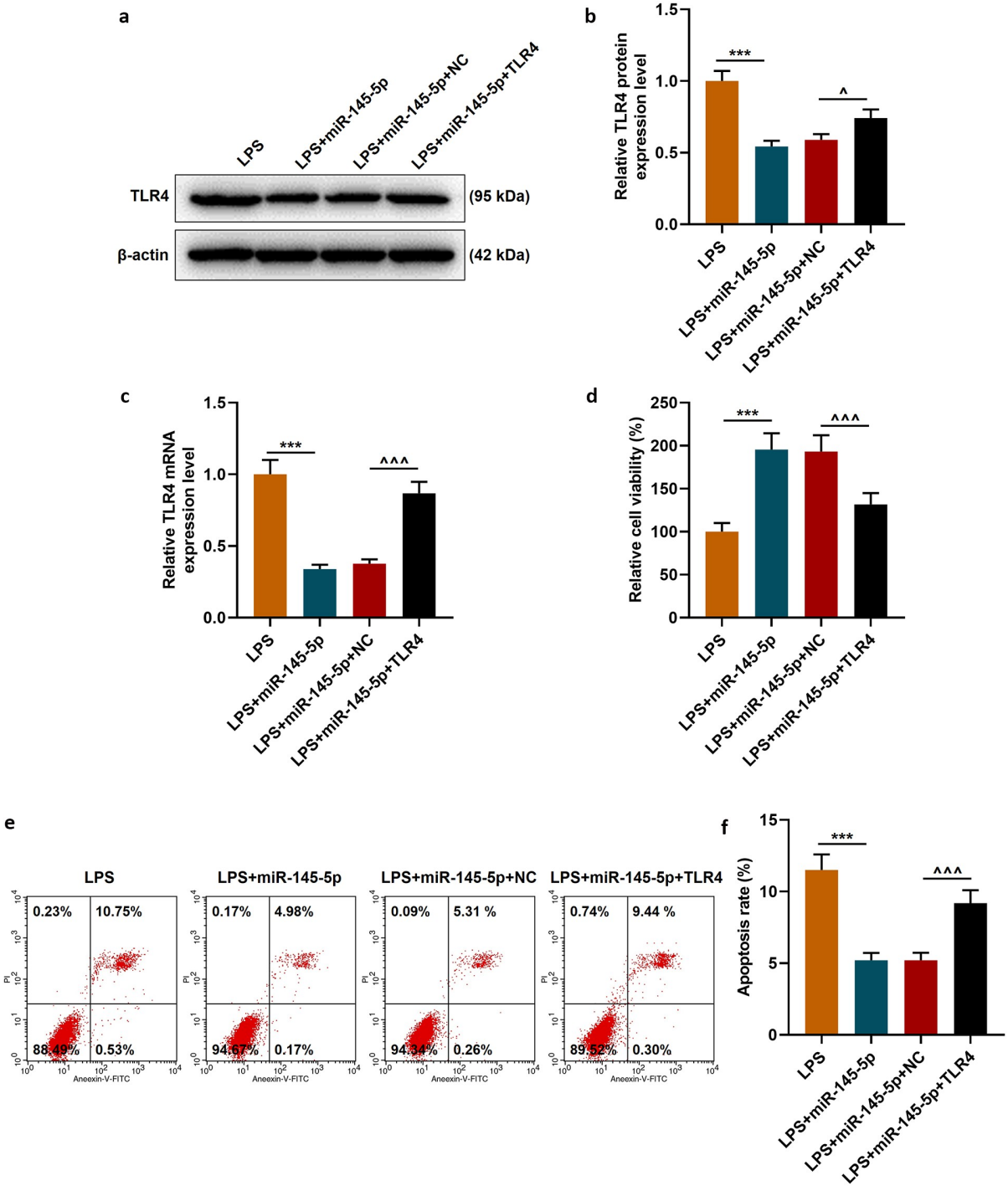

Figure 7. MiR-145-5p inhibited TLR4 expression and TLR4 overexpression significantly reversed the protective effect of EX-miR-145-5p on PC12 cell viability, inhibition of apoptosis.

(a,b) Western blot was used to detect the expression of TLR4 in cells. (c) QRT-PCR was used to detect the expression of TLR4 in cells. (d) MTT was used to detect the viability of PC12 cells transfected with miR-145-5p mimic and TLR4 overexpression vector. (e,f) Flow cytometry was used to detect the apoptosis of PC12 cells transfected with miR-145-5p mimic and TLR4 overexpression vector. (n = 3, ***$P < 0.001$, vs. LPS group; $^{\wedge\wedge\wedge}P < 0.001$, vs. LPS+EX-miR-NC group)

derived EXs, it was found that EXs can deliver miR-146b to glioma cells, inhibit tumor growth, and reduce tumor volume [36]. In addition, EXs can promote the expression of miR-21 in human bronchial epithelial cells, activate STAT3, increase the level of VEGF, promote angiogenesis, and has a closely relation to the occurrence of lung cancer [37]. Similarly, many studies have confirmed that

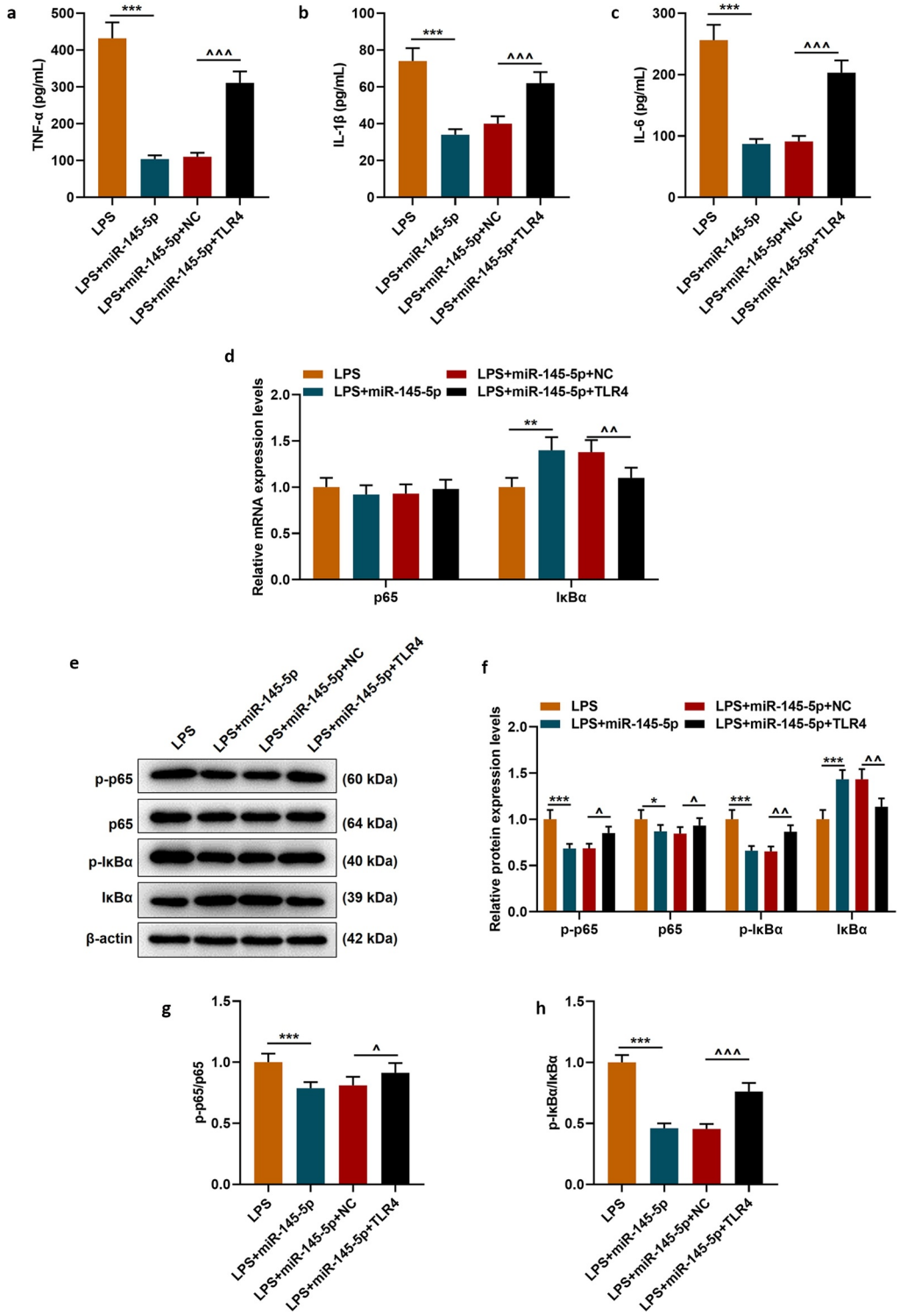

Figure 8. TLR4 overexpression significantly reversed the effect of EX-miR-145-5p on inhibiting inflammatory response and activating TLR4/NF- κB pathway in PC12 cells.

(a) ELISA was used to detect TNF-α expression in PC12 cells transfected with miR-145-5p mimic and TLR4 overexpression vector. (c) ELISA was used to detect IL-1β expression in PC12 cells transfected with miR-145-5p mimic and TLR4 overexpression vector. (c) ELISA was used to detect IL-6 expression in PC12 cells transfected with miR-145-5p mimic and TLR4 overexpression vector. (d) The expressions of p65 and IκBα were detected by qRT-PCR in PC12 cells transfected with miR-145-5p mimic and TLR4 overexpression vector. (e–h) The expressions of p65 and IκBα were detected by Western blot in PC12 cells transfected with miR-145-5p mimic and TLR4 overexpression vector. (n = 3, ***$P < 0.001$, vs. LPS group; ^^$P < 0.01$, ^^^$P < 0.001$, vs. LPS+EX-miR-NC group)

the ability of stem cells to repair damaged organs is closely related to the EXs they secrete.

Based on the above research, we established an SCI rat model to explore the effect of EXs secreted by MSCs transfected with miR-145-5p on functional damage in rats. First of all, we found that EX loaded with miR-145-5p can significantly improve the functional recovery of hind limbs in SCI rats. Histopathological observation also demonstrated that EX loaded with miR-145-5p can not only significantly reduce tissue damage in SCI rats, but also reduce the levels of inflammatory factors in the spinal cord tissue, which indicates that miR-145-5p in MSC-EXs can alleviate the pathogenesis of SCI. At present, TLR4/NF-κB signaling pathway is the most common signaling pathway in studying the molecular mechanisms related to the pathogenesis of SCI [38–40], Shiokarin has been shown to inhibit inflammation induced by SCI by inhibiting the TLR4/NF – B signaling pathway [38]. And therefore, we also tested the effect of EX-miR-145-5p on TLR4/NF -κB signaling pathway related proteins in the SCI rat model. It was found that EX-miR-145-5p can effectively inhibit the activation of TLR4/NF-κB signaling pathway.

Studies have found that miR-145-5p regulates the AKT/GSK signaling pathway by targeting CXCL16, thereby inhibiting the proliferation and inflammatory response of rat mesangial cells [41]. MiR-145-5p is also found to inhibit the occurrence and metastasis of malignant melanoma by targeting TLR4 signaling pathway through NF-κB [42]. In the present study, in order to explore whether EX-miR-145-5p can affect the TLR4/NF-κB signaling pathway to inhibit the occurrence of inflammation and regulate the progress of SCI, we established a PC12 cell model stimulated by LPS. We confirmed that miR-145-5p can specifically bind to TLR4, and through transfection experiments found that overexpression of TLR4 can significantly reverse the protective effect of EX-miR -145-5p on LPS-induced PC12 cell viability and anti-apoptosis, and that EX-miR-145-5p inhibits the production of pro-inflammatory factors. Moreover, overexpression of TLR4 can significantly reverse the effect of EX-miR-145-5p on the activation of the NF-κB pathway. It can be seen that EX-miR-145-5p may improve the progress of SCI by regulating the TLR4/NF-κB signaling pathway. For this reason, we speculate that this may be closely related to EX's mechanism of carrying a large amount of miR-145-5p and enhancing intercellular communication.

In summary, based on the previous research, we suspect that EXs secreted by MSCs can function as a vector for the delivery of miR-145-5p between cells, promote the expression of miR-145-5p and further regulate the expression of its target gene TLR4. Our results indicated that EXs can inhibit the activation of TLR4/NF-κB signaling pathway to inhibit inflammatory response and protect the spinal cord of SCI rats. However, we should also observe the structural characteristics of vesicles more accurately, such as using nanoparticle tracking analysis (NTA) experiments to observe particle size and distribution, and quantitatively analyze foreign bodies.

Disclosure of Conflict-of-Interest

The authors declare no conflicts of interest.

Disclosure statement

No potential conflict of interest was reported by the author(s).

References

[1] Eckert MJ, Martin MJ. Trauma: spinal cord injury. Surg Clin North Am. 2017 Oct;97(5):1031–1045. PubMed PMID: 28958356; eng.

[2] Fakhoury M. Spinal cord injury: overview of experimental approaches used to restore locomotor activity. Rev Neurosci. 2015;26(4):397–405. PubMed PMID: 25870961; eng.

[3] Hota J, Pati SS, Mahapatra PK. Spinal cord self-repair during tail regeneration in Polypedates maculatus and putative role of FGF1 as a neurotrophic factor. J Chem Neuroanat. 2018 Mar;88:70–75. PubMed PMID: 29133075; eng.

[4] Krishnan RV, Muthusamy R, Sankar V. Spinal cord injury repair research: a new combination treatment strategy. Int J Neurosci. 2001;108(3–4):201–207. PubMed PMID: 11699192; eng.

[5] Pearse DD, Bastidas J, Izabel SS, et al. Schwann cell transplantation subdues the pro-inflammatory innate immune cell response after spinal cord injury. Int J Mol Sci. 2018 Aug 28;19(9):2550. PubMed

PMID: 30154346; PubMed Central PMCID: PMCPMC6163303. eng.

[6] Orr MB, Gensel JC. Spinal cord injury scarring and inflammation: therapies targeting glial and inflammatory responses. Neurotherapeutics. 2018 Jul;15 (3):541–553. PubMed PMID: 29717413; PubMed Central PMCID: PMCPMC6095779. eng.

[7] Zhang Y, Zhou Y, Chen S, et al. Macrophage migration inhibitory factor facilitates prostaglandin E(2) production of astrocytes to tune inflammatory milieu following spinal cord injury. J Neuroinflammation. 2019 Apr 13;16(1):85. PubMed PMID: 30981278; PubMed Central PMCID: PMCPMC6461812. eng.

[8] Alizadeh A, Santhosh KT, Kataria H, et al. Neuregulin-1 elicits a regulatory immune response following traumatic spinal cord injury. J Neuroinflammation. 2018 Feb 21;15(1):53. PubMed PMID: 29467001; PubMed Central PMCID: PMCPMC5822667. eng.

[9] Gao L, Dai C, Feng Z, et al. MiR-137 inhibited inflammatory response and apoptosis after spinal cord injury via targeting of MK2. J Cell Biochem. 2018 Apr;119 (4):3280–3292. PubMed PMID: 29125882; eng.

[10] Freria CM, Hall JC, Wei P, et al. Deletion of the fractalkine receptor, CX3CR1, improves endogenous repair, axon sprouting, and synaptogenesis after spinal cord injury in mice. J Neurosci. 2017 Mar 29;37 (13):3568–3587. PubMed PMID: 28264978; PubMed Central PMCID: PMCPMC5373135. eng.

[11] Remsburg C, Konrad K, Sampilo NF, et al. Analysis of microRNA functions. Methods Cell Biol. 2019;151:323–334. .PubMed PMID: 30948016; eng.

[12] Deng G, Gao Y, Cen Z, et al. miR-136-5p regulates the inflammatory response by targeting the IKKβ/NF-κB/A20 pathway after spinal cord injury. Cell Physiol Biochem. 2018;50(2):512–524. PubMed PMID: 30308489; eng.

[13] Yuan M, Zhang L, You F, et al. MiR-145-5p regulates hypoxia-induced inflammatory response and apoptosis in cardiomyocytes by targeting CD40. Mol Cell Biochem. 2017 Jul;431(1–2):123–131. PubMed PMID: 28281187; eng.

[14] Mei LL, Wang WJ, Qiu YT, et al. miR-145-5p suppresses tumor cell migration, invasion and epithelial to mesenchymal transition by regulating the Sp1/NF-κB signaling pathway in esophageal squamous cell carcinoma. Int J Mol Sci. 2017 Aug 23;18(9):1833. PubMed PMID: 28832500; PubMed Central PMCID: PMCPMC5618482. eng.

[15] Wang CY, Yang SH, Tzeng SF. MicroRNA-145 as one negative regulator of astrogliosis. Glia. 2015 Feb;63 (2):194–205. PubMed PMID: 25139829; eng.

[16] De Gasperi R, Graham ZA, Harlow LM, et al. The signature of MicroRNA dysregulation in muscle paralyzed by spinal cord injury includes downregulation of MicroRNAs that target myostatin signaling. PloS One. 2016;11(12):e0166189. PubMed PMID: 27907012; PubMed Central PMCID: PMCPMC5132212. eng.

[17] Yaghoubi Y, Movassaghpour A, Zamani M, et al. Human umbilical cord mesenchymal stem cells derived-exosomes in diseases treatment. Life Sci. 2019 Sep;15(233):116733. . PubMed PMID: 31394127; eng.

[18] Whiteside TL. Exosome and mesenchymal stem cell cross-talk in the tumor microenvironment. Semin Immunol. 2018 Feb;35:69–79. PubMed PMID: 29289420; PubMed Central PMCID: PMCPMC5866206. eng.

[19] Chew JRJ, Chuah SJ, Teo KYW, et al. Mesenchymal stem cell exosomes enhance periodontal ligament cell functions and promote periodontal regeneration. Acta Biomater. 2019 Apr;15(89):252–264. . PubMed PMID: 30878447; eng.

[20] Zhu J, Lu K, Zhang N, et al. Myocardial reparative functions of exosomes from mesenchymal stem cells are enhanced by hypoxia treatment of the cells via transferring microRNA-210 in an nSMase2-dependent way. Artif Cells Nanomed Biotechnol. 2018 Dec;46 (8):1659–1670. PubMed PMID: 29141446; PubMed Central PMCID: PMCPMC5955787. eng.

[21] Roura S, Toward B-GA. Standardization of mesenchymal stromal cell-derived extracellular vesicles for therapeutic use: a call for action. Proteomics. 2019 Jan;19 (1–2):e1800397. PubMed PMID: 30592551; eng.

[22] Yu L, Qu H, Yu Y, et al. LncRNA-PCAT1 targeting miR-145-5p promotes TLR4-associated osteogenic differentiation of adipose-derived stem cells. J Cell Mol Med. 2018 Dec;22(12):6134–6147. PubMed PMID: 30338912; PubMed Central PMCID: PMCPMC6237555. eng.

[23] Basso DM, Beattie MS, Bresnahan JC. Graded histological and locomotor outcomes after spinal cord contusion using the NYU weight-drop device versus transection. Exp Neurol. 1996 Jun;139(2):244–256. PubMed PMID: 8654527; eng.

[24] Gong C, Hu X, Xu Y, et al. Berberine inhibits proliferation and migration of colorectal cancer cells by downregulation of GRP78. Anticancer Drugs. 2020 Feb;31(2):141–149. PubMed PMID: 31743135; eng.

[25] Livak KJ, Schmittgen TD. Analysis of relative gene expression data using real-time quantitative PCR and the 2(-Delta Delta C(T)) Method. Methods. 2001 Dec;25(4):402–408. PubMed PMID: 11846609; eng.

[26] Venkatesh K, Ghosh SK, Mullick M, et al. Spinal cord injury: pathophysiology, treatment strategies, associated challenges, and future implications. Cell Tissue Res. 2019 Aug;377(2):125–151. PubMed PMID: 31065801; eng.

[27] Jorge A, Taylor T, Agarwal N, et al. Current agents and related therapeutic targets for inflammation after acute traumatic spinal cord injury. World Neurosurg. 2019 Dec;132:138–147. PubMed PMID: 31470153; eng.

[28] Wang S, Xu M, Li X, et al. Exosomes released by hepatocarcinoma cells endow adipocytes with tumor-promoting properties. J Hematol Oncol. 2018

Jun 14;11(1):82. PubMed PMID: 29898759; PubMed Central PMCID: PMCPMC6001126. eng.

[29] Hessvik NP, Llorente A. Current knowledge on exosome biogenesis and release. Cell Mol Life Sci. 2018 Jan;75(2):193–208. PubMed PMID: 28733901; PubMed Central PMCID: PMCPMC5756260. eng.

[30] Xin H, Katakowski M, Wang F, et al. MicroRNA cluster miR-17-92 cluster in exosomes enhance neuroplasticity and functional recovery after stroke in rats. Stroke. 2017 Mar;48(3):747–753. PubMed PMID: 28232590; PubMed Central PMCID: PMCPMC5330787. eng.

[31] Xin H, Li Y, Liu Z, et al. MiR-133b promotes neural plasticity and functional recovery after treatment of stroke with multipotent mesenchymal stromal cells in rats via transfer of exosome-enriched extracellular particles. Stem Cells. 2013 Dec;31(12):2737–2746. PubMed PMID: 23630198; PubMed Central PMCID: PMCPMC3788061. eng.

[32] Lankford KL, Arroyo EJ, Nazimek K, et al. Intravenously delivered mesenchymal stem cell-derived exosomes target M2-type macrophages in the injured spinal cord. PloS One. 2018;13(1):e0190358. PubMed PMID: 29293592; PubMed Central PMCID: PMCPMC5749801. eng.

[33] Sun G, Li G, Li D, et al. hucMSC derived exosomes promote functional recovery in spinal cord injury mice via attenuating inflammation. Mater Sci Eng C Mater Bio Appl. 2018 Aug;1(89):194–204. PubMed PMID: 29752089; eng.

[34] Huang JH, Yin XM, Xu Y, et al. Systemic administration of exosomes released from mesenchymal stromal cells attenuates apoptosis, inflammation, and promotes angiogenesis after spinal cord injury in rats. J Neurotrauma. 2017 Dec 15;34(24):3388–3396. PubMed PMID: 28665182; eng.

[35] Lou G, Song X, Yang F, et al. Exosomes derived from miR-122-modified adipose tissue-derived MSCs increase chemosensitivity of hepatocellular carcinoma. J Hematol Oncol. 2015 Oct 29;8(1):122. PubMed PMID: 26514126; PubMed Central PMCID: PMCPMC4627430. eng.

[36] Katakowski M, Buller B, Zheng X, et al. Exosomes from marrow stromal cells expressing miR-146b inhibit glioma growth. Cancer Lett. 2013 Jul 10;335(1):201–204. PubMed PMID: 23419525; PubMed Central PMCID: PMCPMC3665755. eng.

[37] Liu Y, Luo F, Wang B, et al. STAT3-regulated exosomal miR-21 promotes angiogenesis and is involved in neoplastic processes of transformed human bronchial epithelial cells. Cancer Lett. 2016 Jan 1;370(1):125–135. PubMed PMID: 26525579; eng.

[38] Bi Y, Zhu Y, Zhang M, et al. Effect of shikonin on spinal cord injury in rats via regulation of HMGB1/TLR4/NF-kB signaling pathway. Cell Physiol Biochem. 2017;43(2):481–491. PubMed PMID: 28934735; eng.

[39] Ni H, Jin W, Zhu T, et al. Curcumin modulates TLR4/NF-κB inflammatory signaling pathway following traumatic spinal cord injury in rats. J Spinal Cord Med. 2015 Mar;38(2):199–206. PubMed PMID: 24621048; PubMed Central PMCID: PMCPMC4397202. eng.

[40] Chen D, Pan D, Tang S, et al. Administration of chlorogenic acid alleviates spinal cord injury via TLR4/NF-κB and p38 signaling pathway anti-inflammatory activity. Mol Med Rep. 2018 Jan;17(1):1340–1346. PubMed PMID: 29115619; eng.

[41] Wu J, He Y, Luo Y, et al. MiR-145-5p inhibits proliferation and inflammatory responses of RMC through regulating AKT/GSK pathway by targeting CXCL16. J Cell Physiol. 2018 Apr;233(4):3648–3659. PubMed PMID: 29030988; eng.

[42] Jin C, Wang A, Liu L, et al. miR-145-5p inhibits tumor occurrence and metastasis through the NF-κB signaling pathway by targeting TLR4 in malignant melanoma. J Cell Biochem. 2019 Jan 30;120(7):11115–11126. PubMed PMID: 30701576; eng.